Advanced MR Imaging Techniques in the Evaluation of Nonenhancing Gliomas: Perfusion-Weighted Imaging Compared with Proton Magnetic Resonance Spectroscopy and Tumor Grade

NESLIN SAHIN[1,2], ELIAS R. MELHEM[2,3], SUMEI WANG[2], JAROSLAW KREJZA[2,3], HARISH POPTANI[2], SANJEEV CHAWLA[2], GAURAV VERMA[2]

[1] Department of Radiology, Sifa University School of Medicine; İzmir, Turkey
[2] Department of Radiology, University of Pennsylvania; Philadelphia, Pennsylvania, USA
[3] Department of Diagnostic Radiology and Nuclear Medicine, University of Maryland School of Medicine; Baltimore, Maryland, USA

Key words: nonenhancing glioma, MR spectroscopy, perfusion MRI

SUMMARY – *A significant number of nonenhancing (NE) gliomas are reported to be malignant. The purpose of this study was to compare the value of advanced MR imaging techniques, including T2*-dynamic susceptibility contrast PWI (DSC-PWI) and proton magnetic resonance spectroscopy ([1]HMRS) in the evaluation of NE gliomas. Twenty patients with NE gliomas underwent MRI including DSC-PWI and [1]HMRS. The relative CBV (rCBV) measurements were obtained from regions of maximum perfusion. The peak ratios of choline/creatine (Cho/Cr) and myo-inositol/creatine (mIns/Cr) were measured at a TE of 30 ms. Demographic features, tumor volumes, and PWI- and [1]HMRS-derived measures were compared between low-grade gliomas (LGGs) and high-grade gliomas (HGGs). In addition, the association of initial rCBV ratio with tumor progression was evaluated in LGGs. No significant difference was noted in age, sex or tumor size between LGGs and HGGs. Cho/Cr ratios were significantly higher in HGGs (1.7±0.63) than in LGGs (1.2±0.38). The receiver operating characteristic analysis demonstrated that a Cho/Cr ratio with a cutoff value of 1.3 could differentiate between LGG and HGG with a specificity of 100% and a sensitivity of 71.4%. There was no significant difference in the rCBV ratio and the mIns/Cr ratio between LGG and HGG. However, higher rCBV ratios were observed with more rapid progressions in LGGs. The results imply that Cho/Cr ratios are useful in distinguishing NE LGG from HGG and can be helpful in preoperative grading and biopsy guidance. On the other hand, rCBV ratios do not help in the distinction.*

Introduction

Gliomas are the most common form of brain neoplasms and are described in terms of four histologic grades, varying from low-grade to high-grade [1]. Nonenhancing (NE) glial neoplasms are a particularly difficult subgroup to manage. Accurate preoperative grading of these neoplasms has critical impact on decisions related to surgery versus close follow-up, extent of resection, and postoperative treatment. Patient demographics and imaging-based volume of NE glial neoplasms have not been very helpful in preoperatively predicting histological grade [2]. Contrast-enhanced MR imaging has also not been very useful in predicting histological grade as up to 45% of NE gliomas are reported to be malignant [2,3]. Advanced imaging techniques, such as T2*-dynamic susceptibility contrast PWI (DSC-PWI) and proton magnetic resonance spectroscopy ([1]HMRS), provide supplemental information on vascular and meta-

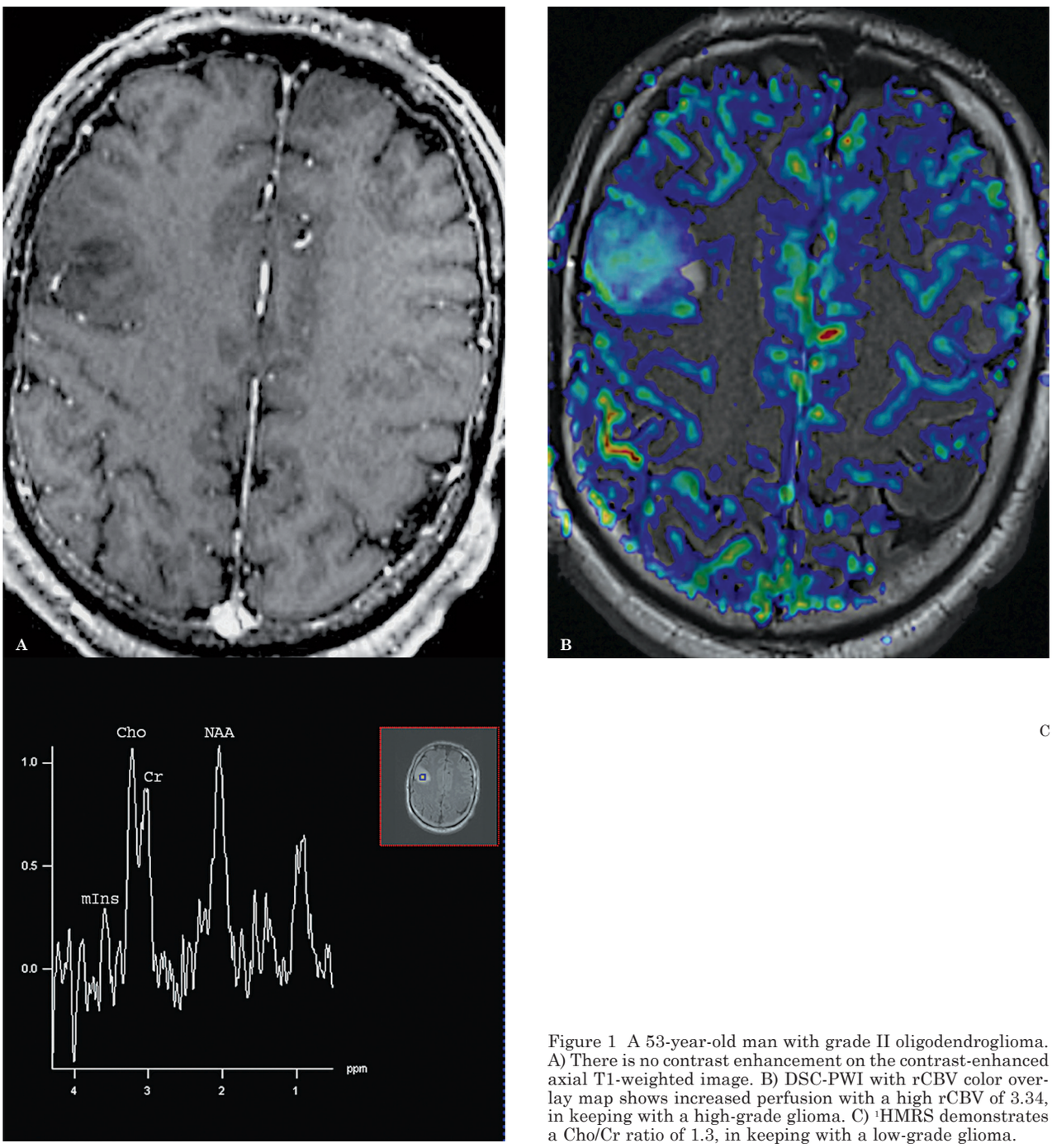

C

Figure 1 A 53-year-old man with grade II oligodendroglioma. A) There is no contrast enhancement on the contrast-enhanced axial T1-weighted image. B) DSC-PWI with rCBV color overlay map shows increased perfusion with a high rCBV of 3.34, in keeping with a high-grade glioma. C) ^{1}HMRS demonstrates a Cho/Cr ratio of 1.3, in keeping with a low-grade glioma.

bolic alterations in NE glial neoplasms, which may improve their preoperative grading [4-6].

The aim of this study was to assess whether or not DSC-PWI and ^{1}HMRS improve the preoperative evaluation of NE gliomas over demographical and conventional MR imaging measures.

Materials and Methods

Subjects

The study protocol was approved by our Institutional Review Board and was compliant with the Health Insurance Portability and Ac-

countability Act. Twenty patients (15 men and five women; mean age, 44.25 years; age range, 28-64 years) with pathologically proven gliomas that had no enhancement on pre-operative contrast-enhanced MR imaging were included in the study. All patients had undergone an MR imaging examination, which included both DSC-PWI and ^{1}HMRS prior to surgery, chemotherapy, or radiation.

The diagnosis was based on open surgery in 14 patients and stereotactic biopsy in five patients after the MR imaging examination. In one of the cases the initial diagnosis was made by biopsy, but the patient underwent surgery after two months and the diagnosis was the same. The neoplasms were classified according to the World Health Organization (WHO) grading system. Patients were divided into two groups depending on their histopathological grade: grade I and II gliomas were considered low-grade gliomas (LGGs) (n = 14), and grade III (n = 6) were considered high-grade gliomas (HGGs).

Acquisition

Conventional MR imaging, DSC-PWI and ^{1}HMRS were performed on a 3T MRI system (Magnetom Trio, Siemens, Erlangen, Germany) equipped with a 12-channel phased-array head coil provided by the manufacturer. The routine imaging protocol included a three-plane scout localizer; axial 3D T1-weighted magnetization-prepared rapid acquisition gradient echo (MPRAGE) images using TR 1760 ms, TE 3.1 ms, TI 950 ms, 192 × 256 matrix size, field of view (FOV) 250 × 250 mm^2, and 1 mm section thickness; axial FLAIR images with TR 9420 ms, TE 141 ms, TI 2500 ms, 192 × 256 matrix size, and 3 mm thick contiguous sections with no gap. Contrast-enhanced axial 3D T1-weighted MPRAGE images were obtained after the acquisition of the DSC-PWI.

DSC-PWI sequences were acquired during the first pass of the standard dose (0.1 mmol/kg) of the intravenous gadopentetate dimeglumine contrast agent (Omniscan, GE Healthcare, Oslo, Norway). 3 mL of contrast agent was injected as a preloading dose at the rate of 2 mL/s. The preloading dose was administered to reduce the effect of contrast agent leakage on the relative CBV (rCBV) measurement. Five minutes after the preloading dose, a bolus dose of contrast agent was injected at a rate of 5 mL/s and immediately followed by a 20 mL bolus injection of normal saline at the same rate. Three mm thick axial sections were acquired through the tumor. The other imaging parameters were as follows: TR/TE = 2000/45 ms, FOV = 22 × 22 cm^2, matrix size = 128 × 128, in-plane resolution = 1.72 × 1.72 × 3 mm^3, and 20 sections. Forty-five images were acquired for each slice with a temporal resolution of 2.1 seconds.

^{1}HMRS data were obtained after administration of the contrast agent. Single-slice two-dimensional (2D) multivoxel ^{1}HMRS was performed using a point-resolved spectroscopy (PRESS) spin echo sequence with water suppression by means of a chemical shift selective saturation (CHESS) sequence. The sequence parameters included the following: TR/TE = 1700/30 ms, number of excitations = 3, FOV = 160 × 160 mm^2 - 200 × 200 mm^2, slice thickness = 15 - 20 mm, bandwidth = 1200 Hz, and matrix size = 16 × 16. The typical voxel size varied from 10 × 10 × 15 mm^3 (volume: 1.5 cm^3) to 10 × 12.5 × 20 mm^3 (volume: 2.5 cm^3) depending on the size of the lesion. The volume of interest (VOI) was defined to include the neoplasm as well as contralateral normal-appearing brain parenchyma, while excluding the scalp, skull base, or sinuses. Eight outer volume saturation slabs (30 mm thick) were placed outside the VOI to suppress lipid signals from the scalp. The data set was acquired using elliptical k-space sampling with weighted phase encoding to reduce the acquisition time. To minimize the effect of increased nominal voxel size by elliptical k-space sampling, a Hamming filter (50%) was applied to the spatial dimensions as recommended in the MRS operator manual provided by Siemens Medical Solutions. Manual shimming was performed to achieve an optimal value of full width at half maximum of the water signal. In general, a shimming of <20 Hz was achieved on the magnitude signal of the water resonance.

Data analysis

Cerebral blood volume maps were reconstructed offline from DSC-PWI data using a PWI task card (The Massachusetts General Hospital, Boston, MA, USA) on a commercial workstation (Leonardo, Syngo Software, Siemens). The procedure used to generate CBV maps from the DSC-MRI data was based on the standard algorithms described previously [7]. The T1 contrast-enhanced images, FLAIR, and CBV maps were converted to Analyze format using MRIcro software (Neuropsychology Lab, Atlanta, GA, USA, http://www.cabiatl.com/mri-

A

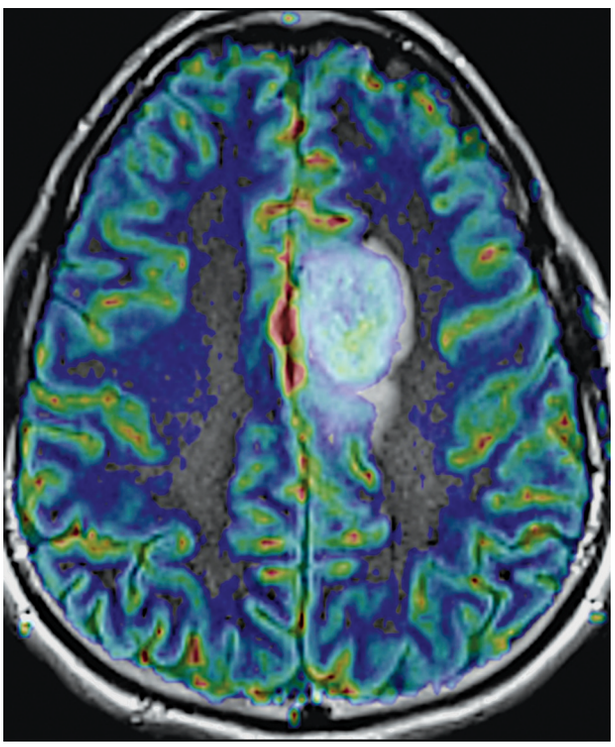

B

C

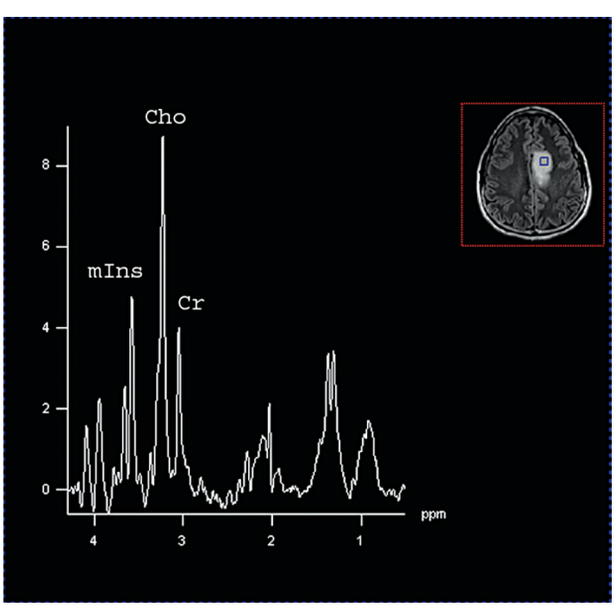

Figure 2 A 35-year-old man with grade III anaplastic oligodendroglioma. A) There is no contrast enhancement on the contrast-enhanced axial T1-weighted image. B) DSC-PWI with rCBV color overlay map shows high perfusion with a rCBV of 3.8, in keeping with a high-grade glioma. C) ^{1}HMRS demonstrates a Cho/Cr ratio of 2.7, in keeping with a high-grade glioma.

cro/mricro/index.html) [8]. The coregistration of CBV maps with FLAIR and contrast-enhanced T1-weighted images was performed using IDL routines (ITT Visual Information Solutions, Boulder, CO, USA) to evaluate the same region of interest (ROI) from all imaging sequences. At least six ROIs (20-30 pixels each) were placed, based on visual inspection, in areas of FLAIR abnormality with apparently highest CBV within the tumor from which maximum CBV (CBV_{max}) values were recorded. This method has been shown to provide the best interobserver and intraobserver reproducibility [9]. The CBV values were normalized by drawing ROIs in the

contralateral normal-appearing white matter (20-30 pixels each) taken as reference to generate relative CBV (rCBV) values. The ROIs were positioned carefully to be placed completely within the apparent margins of the tumor while avoiding contamination from cerebral blood vessels, calcifications, hemorrhages, and CSF spaces. FLAIR images and source images of the DSC-PWI were used to accomplish this.

The region between 0.2 and 4.0 ppm of the spectrum was processed on a short TE of 30 ms. Metabolite peaks were assigned as per convention (ppm): NAA, 2.02 ppm; Cr, 3.02 ppm; Cho, 3.22 ppm; Glx, 2.1–2.5 ppm; mIns, 3.56 ppm; and Lip + Lac, 1.3 ppm. The assignment of these resonances was based on literature values [10]. The signals of Cho, mIns, and Cr were quantified by means of curve fitting. For each spectrum, the acquired signal (free induction decay) was zero-filled (2,048 data points), smoothed (Hamming filter; width = 200 ms), and Fourier-transformed. This was followed by phase (zero and first-order polynomial) and baseline correction for optimal linear frequency dependence. Peak areas were determined offline on a commercial workstation (Leonardo, Syngo Software, Siemens).

The ^{1}HMRS data were analyzed from voxels that exhibited FLAIR hyperintensity. Peak areas of Cho and mIns were normalized with respect to ipsilateral Cr for each voxel. The mean value of creatine was assumed to be an appropriate reference peak to estimate changes in the other metabolites. Metabolic ratios for Cho/Cr and mIns/Cr from all voxels encompassing the FLAIR abnormality, and from the voxels encompassing the contralateral NAWM were calculated. The maximum values were recorded. The maximum ratios of Cho/Cr (Cho/Cr_{max}) and mIns/Cr (mIns/Cr_{max}) were obtained.

The tumor volume was measured based on FLAIR signal abnormalities with the MRIcro software. Regions of interest were traced around FLAIR image abnormalities on each imaging slice, and the total number of pixels encompassing the tumor was calculated. The tumor volume was generated by summing the voxel volumes from all ROIs on individual sections.

We compared the highest rCBV on DSC-PWI and the areas with greatest spectral abnormality on ^{1}HMRS for correspondence. First, we found the area with the highest rCBV on DSC-PWI and the voxel with greatest spectral abnormality on ^{1}HMRS. Then, we analyzed ^{1}HMRS data from voxels exhibiting the highest rCBV on DSC-PWI. The value of blood volume was also measured on the parametric rCBV map corresponding to the areas with greatest spectral abnormality on ^{1}HMRS.

In addition, the association of initial rCBV with tumor progression was determined in patients with low-grade gliomas. We evaluated follow-up MR imaging in three to six month intervals for at least 12 months (12-62 months) and reviewed the clinical charts. We defined progression as one or more new areas of contrast enhancement with or without increase in tumor volume and/or clinically as a development of a new focal deficit or a decline in neurological status.

Results

Representative images from patients with LGGs and HGGs are shown in Figures 1-3. Fourteen patients (70%) were diagnosed with LGG and six patients (30%) with HGG. The final histopathological diagnoses were as follows: grade II, low-grade astrocytomas (n = 5); grade II, low-grade oligodendrogliomas (n = 8); grade II, low-grade mixed oligoastrocytoma (n = 1); grade III, anaplastic astrocytomas (n = 3); grade III, anaplastic oligodendroglioma (n = 1); and grade III, anaplastic oligoastrocytomas (n = 2). Eleven tumors were located in the frontal lobe, one in the temporal lobe, three in the frontoparietal lobes, two in the frontotemporal lobes, one in the temporoparietal lobe, one in the pons, and one in more than two regions of the brain.

The mean age of the LGG patients was 46.86 years (age range: 29-64) while 38.17 years (age range 28-57) was the mean age for HGG patients. The mean volume of FLAIR abnormality was 29.4 cm^3 for LGG and 52 cm^3 for HGG. No significant difference was noted in age, sex, or tumor size between low-grade and high-grade tumors.

On qualitative and quantitative assessments, we found that areas of highest rCBV ratios corresponded to areas with greatest Cho/Cr and mIns/Cr ratios and vice versa. On qualitative assessments, areas of highest rCBV ratios corresponded to areas with greatest Cho/Cr and mIns/Cr ratios. On quantitative assessments, areas of highest rCBV ratios showed greatest Cho/Cr and mIns/Cr ratios and vice versa. The mean $rCBV_{max}$ ratio in LGGs was 1.63±0.78 (range 0.88-3.35) and in HGGs 1.39±1.25 (range 0.73-4.06). There was no significant dif-

A

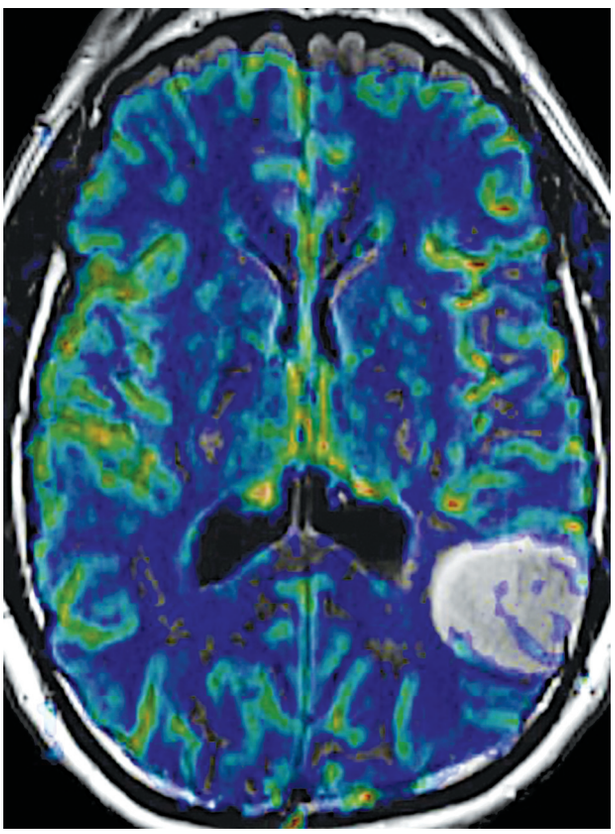

B

C

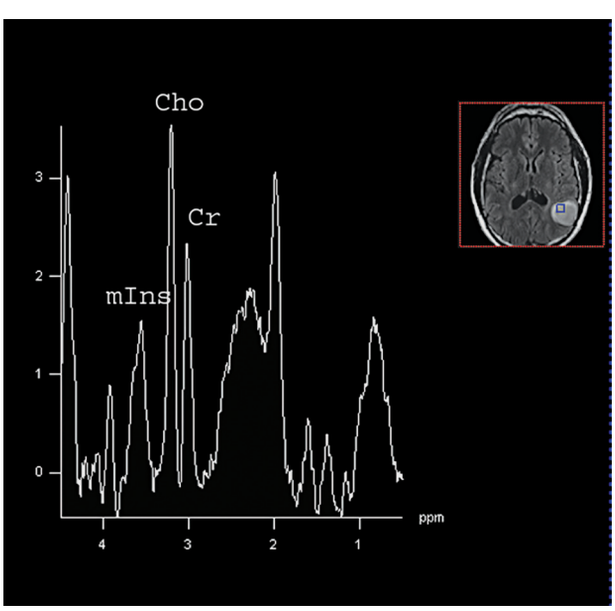

Figure 3 A 37-year-old man with grade III anaplastic oligodendroglioma. A) There is no contrast enhancement on the contrast-enhanced axial T1-weighted image. B) DSC-PWI with rCBV color overlay map shows low perfusion with a rCBV of 0.73, in keeping with a low-grade glioma. C) ^{1}HMRS demonstrates a Cho/Cr ratio of 1.55, in keeping with a high-grade glioma.

ference in the $rCBV_{max}$ ratio between nonenhancing LGGs and HGGs ($P > 0.05$). In LGGs the mean Cho/Cr_{max} ratio was 1.2±0.38 (range 0.8-2.3), and the mean $mIns/Cr_{max}$ ratio was 0.5±0.22 (range 0.22-1.0). In HGGs, the mean Cho/Cr_{max} ratio was 1.7±0.63 (range 1.3-2.8), and the mean $mIns/Cr_{max}$ ratio was 0.53±0.35 (range 0.32-1.28). The Cho/Cr_{max} ratio of HGGs

was significantly higher than that of LGGs ($P > 0.003$; Figure 4). The Cho/Cr_{max} ratio cutoff value of 1.3 could differentiate LGG from HGG with a specificity of 71.4% and a sensitivity of 100.0%. However, differences in $mIns/Cr_{max}$ ratios between the two categories of tumors were not as significant ($P > 0.05$).

There was no significant correlation between the $rCBV_{max}$ ratio and Cho/Cr_{max} and $mIns/Cr_{max}$ ratios.

In seven of the 14 LGGs, the rCBV ratios were higher than 1.63, the mean rCBV ratio of LGGs and three of these LGGs with an initial diagnosis of grade II astrocytoma, progressed to a high grade in six to 15 months. There was no progression in the other four of these LGGs with high rCBV; three grade II oligodendrogliomas and one grade II oligoastrocytoma. On the other hand, two of the LGGs with an initial diagnosis of grade II astrocytoma and low rCBV ratios were stable for at least two years. The patient demographics, histological results, imaging findings, and clinical outcome in LGGs with high rCBV are shown in Table 1.

Discussion

Our study analyzed the $rCBV_{max}$ ratios indicative of tumor vascularity and the Cho/Cr_{max} and $mIns/Cr_{max}$ ratios depicting metabolite alterations within nonenhancing (NE) glial tumors. The qualitative and quantitative assessments demonstrated that areas with the greatest Cho/Cr and mIns/Cr ratios on ^{1}HMRS and areas of highest rCBV ratios on CBV maps corresponded to each other. From the current results of ^{1}HMRS, the Cho/Cr ratios with a cutoff value of 1.3 had a high predictive value with a sensitivity of 71.4% and specificity of 100% for differentiating NE gliomas. All six high-grade gliomas (HGGs) were correctly categorized as high grade using a Cho/Cr cutoff ratio of 1.3.

Advanced imaging techniques such as DSC-PWI and ^{1}HMRS provide supplemental diagnostic information to characterize NE glial neoplasms that may have high-grade components interspersed within them [4-6,11-13]. Although advanced MR imaging techniques have been extensively used in the characterization of gliomas, to the best of our knowledge, few studies have evaluated the value of both ^{1}HMRS and DSC-PWI solely in preoperative grading of NE gliomas.

Choline is related to cell membrane metabolism, and increased levels of choline compounds have been widely associated with malignancy suggesting increased cellularity or cell membrane turnover [10,14-16]. Toyooka et al. [17] demonstrated that the mean Cho/Cr ratio was useful to discriminate between grade II and III gliomas. Furthermore, choline measurements were superior to blood volume information for grading glioma, particularly in differentiating grade II from III that is consistent with our results. Myo-inositol is identified as a singlet on ^{1}HMRS at a short TE ($\leq$ 30 ms), usually assigned at 3.56 ppm [18]. Myo-inositol is mostly located within astrocytes and involved in the activation of protein C kinase which leads to the production of proteolytic enzymes [19]. Castillo et al. [20] reported that levels of mIns/Cr were higher in patients with low-grade astrocytomas that may reflect the fact that the metabolism of mIns is not being up-regulated. They also found an inverse relationship between Cho/Cr and mIns/Cr ratios, with the lowest Cho/Cr ratio seen in low-grade gliomas (LGGs). However, we did not find any statistically significant relationship between the mIns/Cr ratio and the grade of the tumor, and there was no relationship between Cho/Cr and mIns/Cr ratios of NE gliomas.

Previous studies have demonstrated strong positive correlations between rCBV, tumor vascularity, and histopathological grade in cerebral gliomas [2,11,14]. Law et al. [14] reported that the combination of rCBV and Cho information demonstrates high sensitivity and specificity in grading gliomas, but Cho alone showed lower sensitivity and specificity compared with CBV. These findings contrasted with other studies showing that ^{1}HMRS was superior to DSC-PWI in distinguishing benign from malignant brain tumors [16,17]. The clinical utility of perfusion MRI in NE gliomas was studied by Maia et al. [5] who confirmed the correlation between rCBV measurements and histopathological grade similar to the results of a previous study [2]. Batra et al. [6] demonstrated significant differences in the rCBV and the Cho/Cr ratios in NE gliomas, and good correlation was found between the rCBV and the Cho/Cr ratios. However, a single-voxel ^{1}HMRS technique, performed in nearly half of the patients, is subject to greater partial volume contamination. We used a multivoxel ^{1}HMRS that can acquire spectra from numerous voxels to assess different regions of a large tumor to compare with the tumor vascularity on DSC-PWI.

From the current results of DSC-PWI, the difference in rCBV ratios was limited between

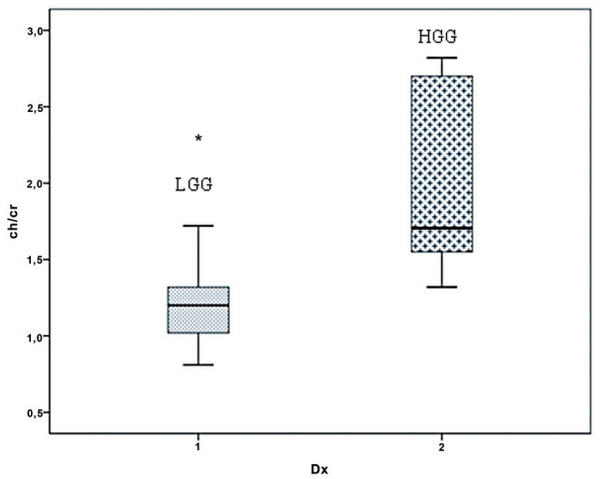

Figure 4 Cho/Cr ratio for low-grade (LGG) and high-grade (HGG) gliomas. The Cho/Cr_{max} ratio of HGGs was significantly higher than that of LGGs (P > 0.003).

Table 1 Patient demographics, histological results, imaging findings, and clinical outcome in LGGs with high rCBV

Patient no.	*Age*	*Sex*	*Histological Results*	*Diagnosis*	*rCBV*	*Cho/Cr*	*Clinical outcome*
1	41	M	LGA	Biopsy	↑ (1.77)	↓ (0.83)	P
2	59	M	LGA	Biopsy	↑ (2.57)	↓ (1.29)	P
3	64	F	LGA	Biopsy	↑ (2.3)	↓ (0.97)	P
4	47	F	LGO	Surgery	↑ (1.79)	↓ (1.09)	S
5	53	M	LGO	Surgery	↑ (3.34)	↓ (1.2)	S
6	53	F	LGO	Surgery	↑ (1.89)	↓ (1.3)	S
7	31	M	LGOA	Surgery	↑ (3.35)	↑ (1.72)	S

rCBV, relative cerebral blood volume; *LGA*, low-grade astrocytoma; *LGO*, low-grade oligodendroglioma; *LGOA*, low-grade oligoastrocytoma; *P*, progressive; *S*, stable.

LGGs and HGGs. Our study demonstrated that low rCBV ratios were also present in NE HGGs. In one of our patients with a low rCBV ratio and a Cho/Cr ratio slightly higher than the cutoff value, initial histopathological diagnosis was grade II, and the final diagnosis in consensus was revised to grade III oligoastrocytoma, with the comment that it was possibly at the low end of this spectrum. But in two of the HGG cases with the lower rCBV ratios (less than 1.0), the Cho/Cr ratios were higher than the cutoff value of 1.3. These findings suggest that malignant histopathological features may have already occurred in these cases including increased cellularity with subtle vascular proliferation.

The dedifferentiation of LGG into HGG is probably a highly variable continuum. At some stage of the malignant transformation of gliomas, the increased proliferation of neoplastic cells may stimulate the vasodilatation of the existing vessels that may precede the onset of angiogenesis, without the expected disruption of the blood-brain barrier. Therefore, rCBV measurements may reveal changes due to vasodilatation as an early predictor of tumor progression. Previous studies supported this hypothesis by showing that glial tumors with high rCBV values were more likely to progress to high-grade gliomas at some point during follow-up [11,21,22]. Seven of the 14 LGGs with benign spectra consistent with the histopathological diagnosis had rCBV ratios higher than 1.75, the threshold value for rCBV found to give the optimal sensitivity and specificity in predicting glioma grade [14]. In addition, all three of these cases with an initial diagnosis of grade II astrocytoma progressed to a high grade with contrast enhancement in six to 15 months. The histopathological diagnosis of another four of these LGGs with high rCBV was oligodendroglioma. Therefore, rCBV maps may improve the

accuracy of biopsies by guiding the biopsy to identify a target for the most malignant areas of the tumor and rCBV measurements can be helpful to identify early malignant transformation in clinical follow-up over that of conventional MR imaging in NE LGGs.

Relative CBV has been reported as an independent predictive factor that probabilistically supports adverse events (either progression or death) [23]. A recent study assumed that spectroscopy data including the Cho/NAA, Lac/Cr, and Lip/Cr ratios probabilistically supported rCBV, but the Cho/Cr ratio was not a predictive factor of rCBV [24]. These findings may explain our results that although a Cho/Cr ratio with a cutoff value 1.3 was correlated with the initial histopathological diagnosis of the tumors, the Cho/Cr ratio was not as helpful in predicting the outcome as the rCBV ratio. Therefore, we conclude that the analysis of other metabolites may provide prognostic information on the clinical outcome as a predictor of adverse events in addition to rCBV ratio.

It is possible that the five NE LGGs which were biopsied may have had an incorrect histopathological diagnosis of tumor grade due to sampling error. One of these five patients was assigned as grade II astrocytoma histopathologically and had low rCBV ratios and benign spectra. This patient was stable clinically and stable on follow-up MR images for at least two years after the initial biopsy, which supported the initial diagnosis and the AI findings. In another patient with grade II oligodendroglioma, the rCBV ratio was lower than 1.75, and the Cho/Cr ratio was higher than 1.3; the patient underwent surgery after one year because of progression, but the diagnosis was the same. Three of the low-grade astrocytomas with high rCBV ratios and benign spectra dedifferentiated to high grade with contrast enhancement. However, it is not clear whether those tumors already had high-grade components at the time of biopsy or if the high rCBV ratio was an indicator of an early vascular proliferation that was undergoing malignant transformation, because histopathological correlation with DSC-PWI findings was not performed on a one-to-one basis for tumor regions.

On the other hand, it was mentioned that oligodendrogliomas tend to have higher perfusion, probably associated with the fine capillary network [11,25]. In our study, there were nine LGGs with oligodendroglial components, and four of them showed rCBV ratios higher than 1.75. The Cho/Cr ratio was 1.3 in one of them and lower than 1.3 in two of them. The oligodendroglial component explains high rCBV ratio and benign spectra in these LGGs. In only one patient with grade II oligoastrocytoma, was the Cho/Cr ratio higher than 1.3; the patient was stable for two years that this was the only case in which both techniques failed to predict the grade. We conclude that ^{1}HMR spectroscopy measurements may be helpful in differentiating oligodendroglial tumor grade similar to a recent study [25].

The current study showed conflicting results between the findings of ^{1}HMRS and DSC-PWI in predicting the grade and outcome of NE gliomas. Our findings suggest that Cho/Cr ratios correlate more accurately with initial histopathological grading than rCBV ratios. From the current results of DSC-PWI, the difference in rCBV ratios was limited between LGGs and HGGs. We aimed to compare the value of AI techniques for the initial evaluation of NE gliomas to improve the clinical management, therefore our study consisted of both oligodendrogliomas and astrocytomas. This may explain the conflicting results with some of the perfusion MRI studies. On the other hand, some of the tumors that were LGG at the histopathological analysis with benign spectra showed high perfusion areas belonging to either premalignant or malignant areas demonstrated in follow-up or oligodendroglial components confirmed with the histopathological analysis. The findings confirm the results of previous studies that rCBV ratios may be better predictors of tumor progression than initial histopathological interpretations. So, especially with large cerebral gliomas, which are often histopathologically heterogeneous with varying grades of malignancy, exact areas of high rCBV ratios can be selectively chosen to reduce sampling errors. It is also important to distinguish oligodendrogliomas from astrocytomas: the subgroup of oligodendrogliomas with allelic loss on chromosomes 1p and 19q have a significantly better prognosis and a particular sensitivity to chemotherapy [26].

However, our preliminary study also has some limitations. We had a small number of patients. We included both oligodendrogliomas and astrocytomas in our study because our primary aim was to differentiate low grade from high grade in NE tumors preoperatively. We found more reliable results with ^{1}HMRS than DSC-PWI for diagnosis of oligodendrogliomas. Further studies may be useful for differentiating oligodendrogliomas and astrocytomas in

NE tumors using advanced imaging with larger groups. Histopathological quantification of cell density and angiogenesis and correlation with DSC-PWI and ^{1}HMR spectroscopic findings were not performed on a one-to-one basis for tumor regions; such a correlation could be of great value to explain high perfusion areas in LGGs. We believe that these advanced imaging methods can reduce sampling errors and the undergrading of tumors. In the present study, we used ^{1}HMRS at a short TE (≤ 30 ms) to evaluate mIns; the difficulty associated with ^{1}HMRS at a short TE is the identification and measurement of individual metabolite contributions [10]. Thus, it may be possible to provide better discrimination with other metabolites such as lipid/lactate at intermediate and long TEs, which were reported as predictive factors of survival. We chose peak-area ratios due to the simplicity of analysis. Absolute metabolite quantification methods may improve the sensitivity and specificity of ^{1}HMRS, but such methods are not easy to use in a clinical setting due to their time-consuming nature and some problems with the techniques. However, our preliminary findings with a small sample of patients provide important data with advanced imaging on the biological behavior of NE tumors. The findings seem to generate a need for more dedicated prospective studies with larger patient populations using ^{1}HMRS and DSC-PWI correlated with histopathological findings and clinical outcomes.

Accurate preoperative grading of NE glial tumors is critical for clinical management because of the diagnostic and therapeutic challenge for patients with an imaging diagnosis of LGG. The current reference standard for determining glioma grade is histopathological assessment. However, grade may not be accurately determined histopathologically due to sampling error and interpathologist and intrapathologist variability in interpretation resulting in tumor undergrading and affecting the clinical management. The current study demonstrated that advanced imaging techniques, including ^{1}HMRS and DSC-PWI, can provide additional data over conventional MR imaging and histopathological diagnosis in such tumors. The areas with high perfusion and/or abnormal spectra within the tumor can be chosen for biopsy to provide accurate tumor grading, and can thus be helpful to plan optimum treatment strategy and to decide whether to administer postoperative adjuvant therapy or to determine the interval of follow-up. Because of the possibility of sampling error, if there is discordance between histopathological grade and findings on ^{1}HMRS and DSC-PWI, lesions with high rCBV ratios and/or abnormal spectra can be considered for adjuvant therapy.

In conclusion, Cho/Cr ratios are useful to distinguish NE LGG from HGG and can be helpful in preoperative grading and biopsy guidance. On the other hand, rCBV ratios do not help in the distinction, but they may be useful for guiding biopsy to identify higher-grade tumor components and predict patient outcome in NE LGG. Our results suggest that advanced imaging techniques including ^{1}HMRS with DSC-PWI provide important supplemental diagnostic information in the clinical management of NE gliomas, not available with conventional imaging.

Acknowledgements

The support of clinical research coordinators Lisa M. Desiderio, Kelly J. Sexton, Matthew Voluck, Mary Giancoli, and technologist Jeffrey Punzalan is gratefully acknowledged.

References

1 Kleihues P, Cavenee WK. Pathology and genetics of tumours of the nervous system. Lyon: International Agency for Research on Cancer; 2000.
2 Morita N, Wang S, Chawla S, et al. Dynamic susceptibility contrast perfusion weighted imaging in grading of nonenhancing astrocytomas. J Magn Reson Imaging. 2010; 32 (4): 803-808.
3 Ginsberg LE, Fuller GN, Hashmi M, et al. The significance of lack of MR contrast enhancement of supratentorial brain tumors in adults: histopathological evaluation of a series. Surg Neurol. 1998; 49 (4): 436-440.
4 Al-Okaili RN, Krejza J, Wang S, et al. Advanced MR imaging techniques in the diagnosis of intraaxial brain tumors in adults. Radiographics. 2006; 26 (Suppl 1): S173-189.
5 Maia AC Jr, Malheiros SM, da Rocha AJ, et al. MR cerebral blood volume maps correlated with vascular endothelial growth factor expression and tumor grade in nonenhancing gliomas. Am J Neuroradiol. 2005; 26 (4): 777-783.
6 Batra A, Tripathi RP, Singh AK. Perfusion magnetic resonance imaging and magnetic resonance spectroscopy of cerebral gliomas showing imperceptible contrast enhancement on conventional magnetic resonance imaging. Australas Radiol. 2004; 48 (3): 324-332.
7 Cha S, Knopp EA, Johnson G, et al. Intracranial mass lesions: dynamic contrast-enhanced susceptibility-weighted echo-planar perfusion MR imaging. Radiology. 2002; 223 (1): 11-29.
8 Rorden C, Brett M. Stereotaxic display of brain lesions. Behav Neurol. 2000; 12 (4): 191-200.
9 Wetzel SG, Cha S, Johnson G, et al. Relative cerebral blood volume measurements in intracranial mass lesions: interobserver and intraobserver reproducibility study. Radiology. 2002; 224 (3): 797-803.
10 Govindaraju V, Young K, Maudsley AA. Proton NMR chemical shifts and coupling constants for brain metabolites. NMR Biomed. 2000; 13 (3): 129-153.
11 Lev MH, Ozsunar Y, Henson JW, et al. Glial tumor grading and outcome prediction using dynamic spin-echo MR susceptibility mapping compared with conventional contrast-enhanced MR: confounding effect of elevated rCBV of oligodendrogliomas. Am J Neuroradiol. 2004; 25 (2): 214-221.
12 McKnight TR, Smith KJ, Chu PW, et al. Choline metabolism, proliferation, and angiogenesis in nonenhancing grades 2 and 3 astrocytoma. J Magn Reson Imaging. 2011; 33 (4): 808-816.
13 Liu X, Tian W, Kolar B, et al. MR diffusion tensor and perfusion-weighted imaging in preoperative grading of supratentorial nonenhancing gliomas. Neuro Oncol. 2011; 13 (4): 447-455.
14 Law M, Yang S, Wang H, et al. Glioma grading: sensitivity, specificity, and predictive values of perfusion MR imaging and proton MR spectroscopic imaging compared with conventional MR imaging. Am J Neuroradiol. 2003; 24 (10): 1989-1998.
15 Castillo M, Kwock L. Proton MR spectroscopy of common brain tumors. Neuroimaging Clin N Am. 1998; 8 (4): 733-752.
16 Fayed N, Modrego PJ. The contribution of magnetic resonance spectroscopy and echoplanar perfusion-weighted MRI in the initial assessment of brain tumors. J Neurooncol. 2005; 72 (3): 261-265.
17 Toyooka M, Kimura H, Uematsu H, et al. Tissue characterization of glioma by proton magnetic resonance spectroscopy and perfusion-weighted magnetic resonance imaging: glioma grading and histological correlation. Clin Imaging. 2008; 32 (4): 251-258.
18 Cerdàn S, Parrilla R, Santoro J, et al. 1H NMR detection of cerebral myo-inositol. FEBS Lett. 1985; 187 (1): 167-172.
19 Danielsen ER, Ross B. Magnetic resonance spectroscopy diagnosis of neurological diseases. New York: Marcel Decker; 1999. p 30-34.
20 Castillo M, Smith JK, Kwock L. Correlation of myo-inositol levels and grading of cerebral astrocytomas. Am J Neuroradiol. 2000; 21 (9): 1645-1649.
21 Law M, Oh S, Babb JS, et al. Low-grade gliomas: dynamic susceptibility-weighted contrast-enhanced perfusion MR imaging - Prediction of patient clinical response. Radiology. 2006; 238 (2): 658-667.
22 Danchaivijitr N, Waldman AD, Tozer DJ, et al. Low-grade gliomas: do changes in rCBV measurements at longitudinal perfusion-weighted MR imaging predict malignant transformation? Radiology. 2008; 247 (1): 170-178.
23 Law M, Oh S, Johnson G, et al. Perfusion magnetic resonance imaging predicts patient outcome as an adjunct to histopathology: a second reference standard in the surgical and nonsurgical treatment of low-grade gliomas. Neurosurgery. 2006; 58 (6): 1099-1107.
24 Guillevin R, Menuel C, Abud L, et al. Proton MR spectroscopy in predicting the increase of perfusion MR imaging for WHO grade II gliomas. J Magn Reson Imaging. 2012; 35 (3): 543-550.
25 Xu M, See SJ, Ng WH, et al. Comparison of magnetic resonance spectroscopy and perfusion-weighted imaging in presurgical grading of oligodendroglial tumors. Neurosurgery. 2005; 56 (5): 919-926.
26 Chawla S, Oleaga L, Wang S, et al. Role of proton magnetic resonance spectroscopy in differentiating oligodendrogliomas from astrocytomas. J Neuroimaging. 2010; 20 (1): 3-8.

Neslin Sahin, MD
Department of Radiology
Sifa University School of Medicine
Fevzipasa Boulevard No. 172/2
35240 Basmane İzmir
Turkey,
Tel.: 90 232 343 44 45
Fax: 90 232 343 56 56
E-mail: neslinshn@gmail.com